

Representing and computing the B-derivative of an EC^r vector field's PC^r flow*

George Council[†], Shai Revzen[‡], and Samuel A. Burden[§]

Abstract. This paper concerns first-order approximation of the piecewise-differentiable flow generated by a class of nonsmooth vector fields. Specifically, we represent and compute the Bouligand (or B-)derivative of the piecewise- C^r flow generated by an event-selected C^r vector field. Our results are remarkably efficient: although there are factorially many “pieces” of the desired derivative, we provide an algorithm that evaluates its action on a given tangent vector using polynomial time and space, and verify the algorithm’s correctness by deriving a representation for the B-derivative that requires “only” exponential time and space to construct. We apply our methods in two classes of illustrative examples: piecewise-constant vector fields and mechanical systems subject to unilateral constraints.

Key words. nonsmooth dynamical system, differential equation with discontinuous right-hand side, first-order approximation, Bouligand derivative, saltation matrix,

AMS subject classifications. 34A36, 65D30, 65D99, 70E99,

1. Introduction. First-order approximations – i.e. derivatives – are a foundational tool for analysis and synthesis in smooth dynamical and control systems. For instance, derivatives play a crucial rôle in: stability via spectral [17, Ch. 8.3] or Lyapunov [35, Ch. 5] methods; controllability via linearization [17, Ch. 8.7] or Frobenius/Chow [35, Ch. 8/Ch. 11] techniques; optimality via stationarity [4, Ch. 1] or Pontryagin [29, Ch. 1] principles; identifiability via adaptation [34, Ch. 2] or Expectation-Maximization [23, Ch. 10] methods. These tools all depend on the existence of a computationally-amenable representation for the first-order approximation of smooth system dynamics – namely, the *Fréchet* (or F-)derivative of the system’s smooth flow [28, Ch. 5.6], which derivative is a continuous linear function of tangent vectors.¹

By definition, nonsmooth systems do not generally enjoy existence (let alone computational amenability) of first-order approximations. Restricting to the class of (so-called [6, Def. 1, 2]) *event-selected* C^r (EC^r) vector fields that (i) are smooth except along a finite number of surfaces of discontinuity and (ii) preclude *sliding* [20, 40] or *branching* [37, Def. 3.11] through a transversality condition, we obtain flows that are piecewise-differentiable [6, Thm. 4] (specifically, *piecewise- C^r* (PC^r) [36, Ch. 4.1]). By virtue of their piecewise-differentiability,

*Submitted to the editors DATE.

Funding: This material is based upon work supported by the U. S. Army Research Laboratory and the U. S. Army Research Office under contract/grant number W911NF-16-1-0158, ARO W911NF-14-1-0573, and ARO MURI W911NF-17-1-0306. It is also supported by U. S. National Science Foundation Cyber-Physical Systems Award #1836819 and National Robotics Initiative Award #1924303.

[†]Department of Mechanical Engineering, Carnegie Mellon University, Pittsburgh, PA, USA (gcouncil@andrew.cmu.edu).

[‡]Department of Electrical Engineering and Computer Science, University of Michigan, Ann Arbor, MI, USA (shrevzen@umich.edu).

[§]Department of Electrical & Computer Engineering, University of Washington, Seattle, WA, USA (sburden@uw.edu, <http://faculty.uw.edu/sburden>).

¹We emphasize both properties of the Fréchet derivative (continuity *and* linearity) since the generalized derivative we consider in what follows will retain one (continuity) while relaxing the other (piecewise-linearity).

these flows admit a first-order approximation, termed the *Bouligand* (or B-)derivative, which derivative is a continuous *piecewise*-linear function of tangent vectors [36, Ch. 3, 4]. This paper is concerned with the efficient representation and computation of this piecewise-linear first-order approximation.

Our contributions are twofold: (i) we construct a representation for the B-derivative of the PC^r flow generated by an EC^r vector field; (ii) we derive an algorithm that evaluates the B-derivative on a given tangent vector. Although there are factorially many “pieces” of the derivative, we (i) represent it using exponential time and space and (ii) compute it using polynomial time and space. In an effort to make our results as accessible and useful as possible, we provide a concise summary of the algorithm in [section 2](#) and apply our methods in [section 3](#) *before* rehearsing the technical background in [section 4](#) needed to derive the representation in [section 5](#) and verify the algorithm’s correctness in [section 6](#).

We emphasize that our methods are most useful when there are more than two surfaces of discontinuity, as representation and computation of first-order approximations in the 1- and 2-surface cases have been investigated extensively [2, 5, 10, 11, 18, 19], and these cases do not benefit from the complexity savings touted above. Previously, we established existence of the piecewise-linear first-order approximation of the flow [6, Rem. 1] and provided an inefficient scheme to evaluate each of its “pieces” [6, Sec. 7] in the presence of an arbitrary number of surfaces of discontinuity. To the best of our knowledge, the present paper contains the first representation for the B-derivative of the PC^r flow of a general EC^r vector field and polynomial-time algorithm to compute it.

2. Algorithm. The goal of this paper is to obtain an algorithm that efficiently computes the derivative of a class of nonsmooth flows. This computational task and our solution are easy to describe, yet verifying the algorithm’s correctness requires significant technical overhead. Thus, the remainder of this section will be devoted to specifying the algorithm and the problem it solves using minimal notation and terminology. Subsequent sections will provide technical details – which may be of interest in their own right – that prove the algorithm is correct.

Given vector field $F : \mathbb{R}^d \rightarrow T\mathbb{R}^d$ and trajectory $x : [0, \infty) \rightarrow \mathbb{R}^d$ satisfying²

$$(2.1) \quad \forall t \geq 0 : x_t = \int_0^t F(x_\tau) d\tau,$$

our goal is to approximate how x_t varies with respect to x_0 to first order for a given $t > 0$. Formally, with $\phi : [0, \infty) \times \mathbb{R}^d \rightarrow \mathbb{R}^d$ denoting the *flow* of F satisfying

$$(2.2) \quad \forall t \geq 0, x_0 \in \mathbb{R}^d : \phi_t(x_0) = \int_0^t F(\phi_\tau(x_0)) d\tau,$$

our goal is to evaluate the directional derivative $D\phi_t(x_0; \delta x_0)$ given $t > 0$, $\delta x_0 \in T_{x_0}\mathbb{R}^d$:

$$(2.3) \quad \forall t > 0, \delta x_0 \in T_{x_0}\mathbb{R}^d : D\phi_t(x_0; \delta x_0) = \lim_{\alpha \rightarrow 0^+} \frac{1}{\alpha} (\phi_t(x_0 + \alpha \delta x_0) - \phi_t(x_0)).$$

Specifically, we seek to evaluate this derivative for vector fields that are smooth everywhere except a finite collection of surfaces where they are allowed to be discontinuous. We will

²In this section, we will denote time dependence using subscripts rather than parentheses.

first recall how to obtain the derivative in the presence of zero (subsection 2.1) and one (subsection 2.2) surfaces of discontinuity before presenting our algorithm, which is applicable in the presence of an arbitrary number of surfaces of discontinuity (subsection 2.3).

2.1. Continuously-differentiable vector field. If F is continuously differentiable on the trajectory x , the derivative $\delta x_t = D\phi_t(x_0; \delta x_0)$ satisfies the linear time-varying *variational equation* [27, Appendix B]

$$(2.4) \quad \forall t \geq 0 : \delta x_t = \int_0^t DF(x_\tau) \cdot \delta x_\tau d\tau,$$

whence $\delta x_t = D\phi_t(x_0; \delta x_0)$ can be approximated to any desired precision in polynomial time by applying numerical simulation algorithms [27, Ch. 4] to (2.1), (2.4).

2.2. Single surface of discontinuity. If F is continuously differentiable everywhere except a smooth codimension-1 submanifold $H \subset \mathbb{R}^d$ that intersects the trajectory x transversally at only one point x_s , $s \in (0, t)$, the continuous-time equation (2.4) is augmented by the discrete-time update [2, Eqn. (58)],

$$(2.5) \quad \delta x_s^+ = \left(I_d + \frac{(F^+ - F^-) \cdot \eta^\top}{\eta^\top \cdot F^-} \right) \cdot \delta x_s^- = M \cdot \delta x_s^-,$$

where $\delta x_s^\pm = \lim_{\tau \rightarrow s^\pm} \delta x_\tau$ and $F^\pm = \lim_{\tau \rightarrow s^\pm} F(x_\tau)$ denote the limiting values of δx_τ and $F(x_\tau)$ at s from the right (+) and left (-) and $\eta \in \mathbb{R}^d$ is any vector orthogonal to surface H at x_s ; $M \in \mathbb{R}^{d \times d}$ is termed the *saltation matrix* [10, Eqn. (2.76)], [22, Eqn. (7.65)]. Overall, the desired derivative is

$$(2.6) \quad D\phi_t(x_0; \delta x_0) = D\phi_{t-s}(x_s) \cdot M \cdot D\phi_s(x_0) \cdot \delta x_0,$$

where $D\phi_{t-s}(x_s), D\phi_s(x_0) \in \mathbb{R}^{d \times d}$ can be approximated by simulating (2.2), (2.4) since the flow is smooth away from time s . Computing the saltation matrix M requires $O(d^2)$ time and space, but evaluating its action on δx_s^- in (2.5) requires only $O(d)$ time and space.

2.3. Multiple surfaces of discontinuity. If F is continuously differentiable everywhere except a finite set of smooth codimension-1 submanifolds $\{H_j\}_{j=1}^n$ that intersect the trajectory x transversally at only one point x_s (see Figure 2.1(a) for an illustration when $n = 2$), $s \in (0, t)$, we showed in [6, Eqn. (65)] that the discrete-time update (2.5) is applied once for each surface. However, the order in which the updates are applied, and the limiting values of the vector field used to determine each update's saltation matrix, depend on δx_0 . If the surfaces intersect transversally, there are $n!$ different saltation matrices determined by 2^n vector field values, so considering all update orders requires factorial time and space. To make these observations precise and specify the notation employed in Figures 2.1 and 2.2, we formally define the class of nonsmooth vector fields considered in this paper [6, Defs. 1, 2]:

Definition 2.1. (*event-selected C^r (EC^r) vector field*) A vector field $F : D \rightarrow TD$ defined on an open domain $D \subset \mathbb{R}^d$ is event-selected C^r with respect to $h \in C^r(U, \mathbb{R}^n)$ at $\rho \in \mathbb{R}^d$ if $U \subset D$ is an open neighborhood of ρ and:

1. (*event functions*) there exists $f > 0$ such that $Dh(x) \cdot F(x) \geq f$ for all $x \in U$;

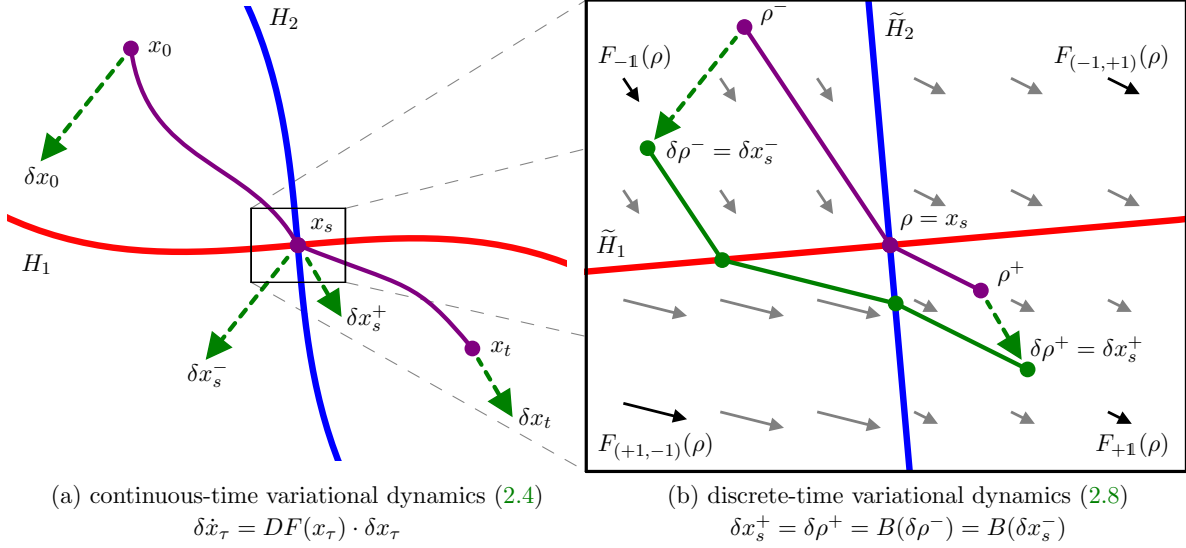


Figure 2.1. Variational dynamics that determine the B-derivative of an EC^r vector field's PC^r flow (2.8). (a) Vector field $F : \mathbb{R}^2 \rightarrow T\mathbb{R}^2$ is smooth everywhere except the smooth codimension-1 submanifolds $H_1, H_2 \subset \mathbb{R}^2$ that intersect transversally at $x_s \in \mathbb{R}^2$, generating a piecewise-differentiable flow $\phi : [0, \infty) \times \mathbb{R}^2 \rightarrow \mathbb{R}^2$ satisfying $\phi_\tau(x_0) = x_\tau$ for all $\tau \in [0, t]$, i.e. F is EC^r and ϕ is PC^r [6]. The B-derivative $D\phi_t(x_0; \delta x_0) = \delta x_t$ is determined as in (2.10) by the continuous-time variational dynamics $\delta \dot{x}_\tau = DF(x_\tau) \cdot \delta x_\tau$ and the discrete-time variational dynamics $\delta x_s^+ = B(\delta x_s^-)$. The algorithms in Figure 2.2 evaluate the piecewise-linear function B using the auxiliary nonsmooth system in (b) determined by the tangent planes \tilde{H}_1, \tilde{H}_2 and vector field limits $F_b(\rho)$ in (2.9) for $b \in \{(-1, (+1, -1), (-1, +1), +1)\} = \{-1, +1\}^2$.

2. (smooth extension) for all $b \in \{-1, +1\}^n = B_n$, with

$$(2.7) \quad D_b = \{x \in U : b_j(h_j(x) - h_j(\rho)) \geq 0\},$$

$F|_{\text{Int } D_b}$ admits a C^r extension $F_b : U \rightarrow TU$.

Our algorithms in Figure 2.2 compute

$$(2.8) \quad \delta x_s^+ = \delta \rho^+ = B(\delta \rho^-) = B(\delta x_s^-)$$

given $\delta \rho^- = \delta x_s^- \in \mathbb{R}^d$, normals $\{\eta_j = Dh_j(\rho)\}_{j=1}^n \subset \mathbb{R}^d$ at x_s to surfaces $\{H_j = h_j^{-1}(\rho)\}_{j=1}^n$, and a function $\Gamma : \{-1, +1\}^n \rightarrow \mathbb{R}^d$ that evaluates limits of the vector field F at $\rho = x_s$,

$$(2.9) \quad \forall b \in \{-1, +1\}^n : \Gamma(b) = F_b(\rho),$$

using the piecewise-constant dynamics illustrated in Figure 2.1(b), which are the discrete-time analog of the continuous-time variational dynamics (2.4). Overall, the desired derivative is

$$(2.10) \quad D\phi_t(x_0; \delta x_0) = D\phi_{t-s}(x_s) \cdot B(D\phi_s(x_0) \cdot \delta x_0),$$

Algorithm 2.1 $\delta\rho^+ \leftarrow B(\delta\rho^-, \eta, \Gamma)$

```

1:  $\delta t \leftarrow 0 \in \mathbb{R}$ 
2:  $\delta\rho^+ \leftarrow \delta\rho^- \in \mathbb{R}^d$ 
3:  $b \leftarrow -\mathbf{1} \in \{-1, +1\}^n$ 
4: while  $b \neq +\mathbf{1}$  do
5:   for  $j \in \{1, \dots, n\}$  do
6:      $\tau_j \leftarrow -\left(\eta_j^\top \cdot \delta\rho^+\right) / \left(\eta_j^\top \cdot \Gamma(b)\right)$ 
7:      $j^* \leftarrow \arg \min_{j \in \{1, \dots, n\}} \{\tau_j : b_j < 0\}$ 
8:      $\delta t \leftarrow \delta t + \tau_{j^*}$ 
9:      $\delta\rho^+ \leftarrow \delta\rho^+ + \tau_{j^*} \cdot \Gamma(b)$ 
10:     $b_{j^*} \leftarrow +1$ 
11: return  $\delta\rho^+ - \delta t \cdot \Gamma(+\mathbf{1})$ 

```

Algorithm 2.2 $\text{def } B(\text{dx}, e, G)$:

```

1:  $\text{dt} = 0$ 
2:  $\text{dx} = \text{np.array}(\text{dx})$ 
3:  $\text{b} = -\text{np.ones}(\text{len}(e), \text{dtype}=\text{np.int})$ 
4: while  $\text{np.any}(\text{b} < 0)$  :
5:    $\text{tau} = -\text{np.dot}(e, \text{dx}) / \text{np.dot}(e, G(\text{b}))$ 
6:    $\text{tau}[\text{b} > 0] = \text{np.inf}$ 
7:    $\text{j} = \text{np.argmin}(\text{tau})$ 
8:    $\text{dt} += \text{tau}[\text{j}]$ 
9:    $\text{dx} += \text{tau}[\text{j}] * G(\text{b})$ 
10:   $\text{b}[\text{j}] = +1$ 
11: return  $\text{dx} - \text{dt} * G(\text{b})$  #  $\text{b} == [+1, \dots, +1]$ 

```

Figure 2.2. Algorithms that evaluate the B-derivative of an EC^r vector field's PC^r flow written in pseudocode (Algorithm 2.1) and Python [30] sourcecode (Algorithm 2.2; requires import numpy as np [25]). These algorithms apply at a point $\rho \in \mathbb{R}^d$ where a vector field $F : \mathbb{R}^d \rightarrow T\mathbb{R}^d$ is event-selected C^r with respect to n surfaces (see Figure 2.1 for an illustration when $d = n = 2$), and assume the following data is given:

<i>tangent direction,</i>	$\delta\rho^- \in T_\rho\mathbb{R}^d,$	$\text{dx} - \text{array}, \text{dx.shape} == (d,);$
<i>surface normals at ρ,</i>	$\eta = \{\eta_j\}_{j=1}^n \subset \mathbb{R}^d,$	$e - \text{array}, e.\text{shape} == (n, d);$
<i>vector field limits (2.9),</i>	$\Gamma : \{-1, +1\}^n \rightarrow \mathbb{R}^d,$	$G - \text{function}, G(\text{b}).\text{shape} == (d,).$

where $B : T_\rho\mathbb{R}^d \rightarrow T_\rho\mathbb{R}^d$ is the continuous piecewise-linear function defined by our algorithms in Figure 2.2. Our algorithms require $O(n^2d)$ time and $O(d)$ space to evaluate the directional derivative (2.3)³.

Assuming for the moment that these algorithms are correct, we emphasize that they achieve a dramatic reduction in the computational complexity of evaluating the B-derivative – from factorial to low-order polynomial – relative to naïve enumeration of all pieces of the B-derivative. However, despite the apparent simplicity of our algorithms (computationally and conceptually), verifying their correctness requires significant technical effort; the bulk of the present paper is devoted to this verification task.

3. Applications. To illustrate and validate our methods, we apply the algorithm from the preceding section to piecewise-constant vector fields in subsection 3.1 and mechanical systems subject to unilateral constraints in subsection 3.2. Sourcecode implementation of Algorithm 2.2 and applications from the remainder of this section are provided in SM.

3.1. Piecewise-constant vector field. Consider the vector field $F : \mathbb{R}^d \rightarrow T\mathbb{R}^d$ defined by

$$(3.1) \quad \dot{x} = F(x) = \mathbf{1} + \Delta(\text{sign}(x))$$

³These algorithms can be modified as in (6.9) to determine the order of surface crossings for the perturbed trajectory without changing the time or space complexity, so the associated saltation matrix (6.4) can be constructed in $O(nd^2)$ time and $O(d^2)$ space; this construction is discussed in more detail in section 6.

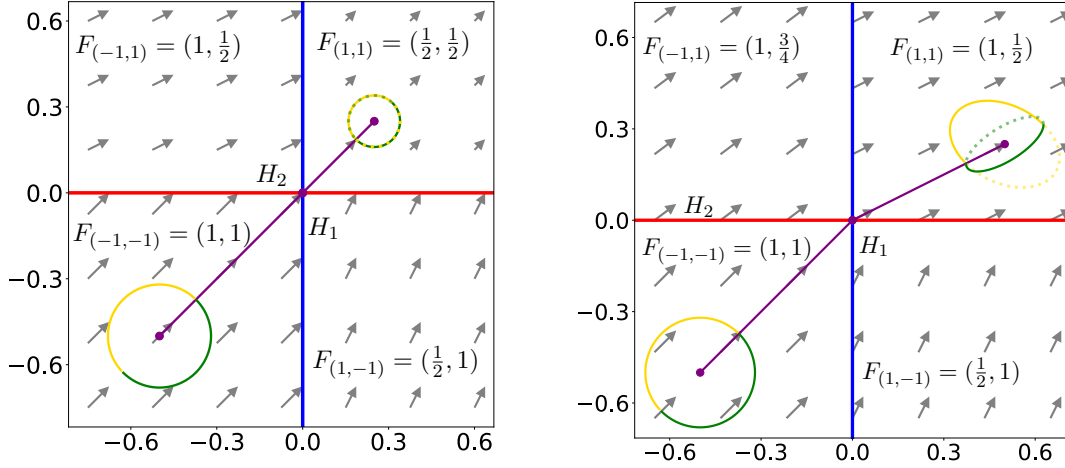


Figure 3.1. B-derivative of vector field from subsection 3.1 in linear (left) and piecewise-linear (right) cases. The vector field F defined in (3.1) is piecewise-constant and discontinuous across the coordinate hyperplanes H_1, H_2 , generating a piecewise-differentiable flow ϕ with B-derivative B . (left) The B-derivative is linear in the special case defined by (3.2). (right) The B-derivative is continuous and piecewise-linear in general, so a ball of initial conditions flows to a piecewise-ellipsoid (gold and green fill).

where $\Delta : B_d \rightarrow \mathbb{R}^d$; so long as all components of all vectors specified by Δ are larger than -1 , i.e. $\min_{b \in B_d} [\Delta(b)]_j > -1$, F is event-selected C^∞ with respect to the identity function $h : \mathbb{R}^d \rightarrow \mathbb{R}^d$ defined by $h(q) = q$. We regard (3.1) as a canonical form for piecewise-constant event-selected C^∞ vector fields that are discontinuous across d subspaces, since any such vector field can be obtained by applying a linear change-of-coordinates to (3.1). In what follows, we focus on the trajectory that passes through the origin $\rho = 0$, which lies at the intersection of d surfaces of discontinuity for F . With $\rho^- = \rho - \frac{1}{2}F_{-1}(\rho)$, $\rho^+ = \rho + \frac{1}{2}F_{+1}(\rho)$, we note that ρ^- flows to ρ^+ through ρ in 1 (one) unit of time.

Our goal is to compute $D_x\phi(1, \rho^-; \delta\rho^-) \in T_{\rho^+}\mathbb{R}^d$ for a given $\delta\rho^- \in T_{\rho^-}\mathbb{R}^d$. In the general case, the desired derivative is piecewise-linear with (up to) $d!$ distinct pieces, providing a general test. In the special case where $\Delta(b) = -\delta \cdot b$ for all $b \in B_d$, $|\delta| < 1$, the desired derivative is linear [6, Eqn. (86)],

$$(3.2) \quad D_x\phi(1, \rho^-; \delta\rho^-) = \frac{1 - \delta}{1 + \delta} \cdot \delta\rho^-,$$

providing a closed-form expression for comparison. Figure 3.1 illustrates results from both cases with $d = 2$; a more exhaustive test suite is provided in SM.

3.2. Mechanical systems subject to unilateral constraints. Consider a mechanical system whose configuration is subject to one-sided (i.e. *unilateral*) constraints. The dynamics of such systems have been studied extensively using the formalisms of complementarity [24, Sec. 3], measure differential inclusions [3, Sec. 3], hybrid systems [21, Sec. 2.4, 2.5], and geometric mechanics [13, Sec. 3]. Regardless of the chosen formalism, in a coordinate chart

$Q \subset \mathbb{R}^d$ the dynamics governing q take the form⁴

$$(3.3) \quad M(q)\ddot{q} = f(q, \dot{q}) \text{ subject to } a(q) \geq 0$$

where: $M(q) \in \mathbb{R}^{d \times d}$ specifies the kinetic energy metric; $f(q, \dot{q}) \in \mathbb{R}^d$ specifies the internal, applied, and Coriolis forces; $a(q) \in \mathbb{R}^n$ specifies the *unilateral constraints*; and we assume in what follows that M , f , and a are smooth functions. Different formalisms enforce the constraint $a(q) \geq 0$ in (3.3) differently, so we consider several cases in the following subsections. Additional illustrative examples are provided in SM.

3.2.1. Rigid constraints yield discontinuous flows. If constraints are enforced *rigidly* as in [3, 21, 24], meaning that they must be satisfied exactly, then the velocity must undergo impact (i.e. change discontinuously) whenever $\dot{q} \in T_q Q$ is such that $a_j(q) = 0$ and $Da_j(q) \cdot \dot{q} < 0$ for some $j \in \{1, \dots, n\}$ [24, Sec. 2] [21, Eqn. (23)] [3, Eqn. (23)]. Unfortunately for our purposes, these discontinuities in the state vector $x = (q, \dot{q})$ cannot be modeled using an event-selected C^r vector field $\dot{x} = F(x)$, and the flow of such systems is generally discontinuous⁵.

3.2.2. Soft conservative constraints yield Lipschitz vector fields, C^1 flows. We now consider the formalism in [13] that “softens” (i.e. approximately enforces) rigid constraints $a(q) \geq 0$ by augmenting the potential energy with *penalty functions* $\{v_j\}_{j=1}^n$ that scale quadratically with the degree of constraint violation [13, Eqn. (12)],

$$(3.4) \quad \forall j \in \{1, \dots, n\} : v_j(q) = \begin{cases} 0, & a_j(q) \geq 0 \\ \frac{1}{2}\kappa_j a_j^2(q), & a_j(q) < 0 \end{cases}$$

In essence, each rigid constraint $a_j(q) \geq 0$ is replaced by a spring with stiffness κ_j , leading to the unconstrained dynamics [13, Eqn. (14)]

$$(3.5) \quad \begin{aligned} M(q)\ddot{q} &= f(q, \dot{q}, u) - \sum_{j=1}^n Dv_j(q)^\top \\ &= f(q, \dot{q}, u) - \sum \left\{ (\kappa_j a_j(q)) \cdot Da_j(q)^\top : j \in \{1, \dots, n\}, a_j(q) < 0 \right\}. \end{aligned}$$

As shown by [39, Thm. 3], trajectories of (3.5) converge to those of (3.3) in the rigid limit (i.e. as stiffnesses go to infinity). Importantly for our purposes, the dynamics in (3.5) can be modeled using an event-selected vector field along trajectories that pass transversally through the constraint surfaces, whence our algorithms can compute the B-derivative of the flow. However, the vector field (3.5) in this case is (locally Lipschitz) continuous, hence the B-derivative is trivial (all non-identity terms in (6.4) are zero), whence the flow is continuously-differentiable (C^1).

⁴We interpret the inequality $a(q) \geq 0$ componentwise.

⁵We note that the flow can be PC^r at non-impact times if the constraint surfaces intersect orthogonally [26], i.e. if the surface normals are orthogonal with respect to the inverse of the kinetic energy metric [3, Theorem 20].

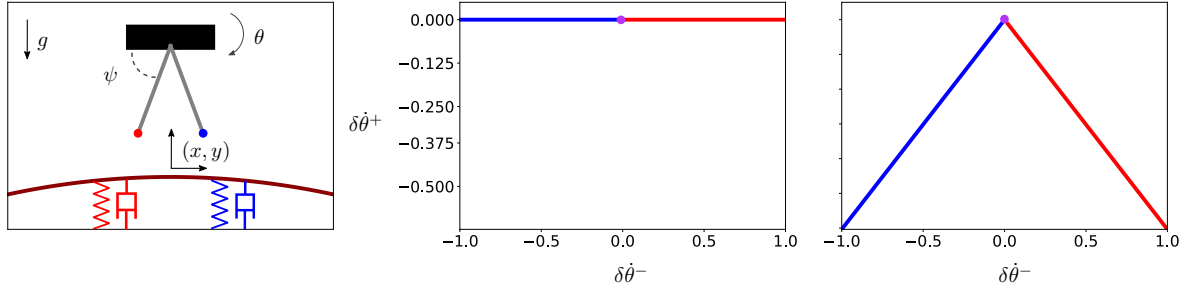


Figure 3.2. Vertical-plane biped, a mechanical system subject to unilateral constraints (subsection 3.2.4), consists of a body with two rigid massless legs falling under the influence of gravity toward a substrate. The system’s flow can be C^1 (left column) or PC^r (right) depending on how forces vary as limbs contact substrate.

3.2.3. Soft dissipative constraints yield EC^r vector fields, C^1 flows. We now augment the unconstrained dynamics (3.5) with dissipation as in [13]:

(3.6)

$$M(q)\ddot{q} = f(q, \dot{q}, u) - \sum \left\{ (\kappa_j a_j(q) + \beta_j Da_j(q) \cdot \dot{q}) \cdot Da_j(q)^\top : j \in \{1, \dots, n\}, a_j(q) < 0 \right\};$$

in essence, each constraint penalty is augmented by a spring-damper that is only active when the constraint is violated as in studies involving contact with complex geometry [12] or terrain [1]. The dynamics in (3.6) can be modeled using an event-selected vector field along trajectories that pass transversally through the constraint surfaces, and the vector field is discontinuous along the constraint surfaces. However, we can show that the flow of (3.6) is continuously-differentiable (C^1) along *any* trajectory that passes transversally through constraint surfaces. Indeed, letting $x = (q, \dot{q})$ denote the state of the system so that $\dot{x} = (\dot{q}, \ddot{q}) = F(x)$ is determined by (3.6), the saltation matrix (2.5) associated with each constraint a_j has the form

$$(3.7) \quad I + \frac{1}{Da_j(q) \cdot \dot{q}} \begin{bmatrix} 0 \\ \pm (\kappa_j a_j(q) + \beta_j Da_j(q) \cdot \dot{q}) \cdot Da_j(q)^\top \end{bmatrix} \begin{bmatrix} Da_j(q) & 0 \end{bmatrix}$$

where the sign in the column vector is determined by whether the constraint is activating (−) or deactivating (+). Since matrices of the form in (3.7) commute, the saltation matrices associated with simultaneous activation and/or deactivation of multiple constraints are all equal, whence the flow of (3.6) is continuously-differentiable (C^1) along any trajectory that passes transversally through constraint surfaces.

3.2.4. Example (vertical-plane biped). To ground the preceding observations, we consider the vertical-plane biped illustrated in Figure 3.2(left) that falls under the influence of gravity toward a substrate. The biped body has mass m and moment-of-inertia J ; we let $(x, y) \in \mathbb{R}^2$ denote the position of its center-of-mass in the plane and $\theta \in S^1$ denote its rotation. Two rigid massless limbs of length ℓ protrude at an angle of $\pm\psi$ with respect to vertical from the body’s center-of-mass above a smooth substrate whose height is a quadratic function of horizontal position, yielding unilateral constraints

$$(3.8) \quad \begin{aligned} a_1(x, y, \theta) &= -y - (x + \ell \cos(\theta - \psi))^2 - \ell \sin(\theta - \psi), \\ a_2(x, y, \theta) &= -y - (x + \ell \cos(\theta + \psi))^2 - \ell \sin(\theta + \psi). \end{aligned}$$

We consider the smoothness of the system's flow along a trajectory that activates both constraints simultaneously⁶. Direct calculation⁷ shows that adopting the formalism in (3.6) yields continuously-differentiable flow for this system as illustrated in Figure 3.2(*middle*).

To obtain a flow that is piecewise-differentiable but *not* continuously-differentiable, we modify the damping coefficients in (3.6) using the following logic⁸: $\beta_1 = \beta_2 = \frac{1}{2}$ if $a_1(q) < 0$ or $a_2(q) \geq 0$ (*exclusive or*); $\beta_1 = \beta_2 = 1$ if $a_1(q) < 0$ and $a_2(q) < 0$. Direct calculation⁷ shows that the saltation matrices obtained from different sequences of constraint activations (left foot reaches substrate before right foot or vice-versa) are distinct:

$$(3.9) \quad M_{(\text{left},\text{right})} - M_{(\text{right},\text{left})} = \begin{bmatrix} 0 & 0 & 0 & 0 & 0 & 0 & 0 \\ 0 & 0 & 0 & 0 & 0 & 0 & 0 \\ 0 & 0 & 0 & 0 & 0 & 0 & 0 \\ 0 & 0 & 0 & 0 & 0 & 0 & 0 \\ -4\beta \cos(\psi) & 0 & -2\beta(\sin(2\psi) + \cos(\psi)) & 0 & 0 & 0 & 0 \\ 0 & 0 & 0 & 0 & 0 & 0 & 0 \end{bmatrix}.$$

The piecewise-linear B-derivative of the system's flow is illustrated in Figure 3.2(*right*).

4. Background. To verify correctness of the algorithms specified in section 2, we utilize the representation of piecewise-affine functions from [15], elements of the theory of piecewise-differentiable functions from [36], and results about the class of nonsmooth flows under consideration from [6]. In an effort to make this paper self-contained (i.e. to save the reader from needing to cross-reference multiple citations to follow our derivations), we include a substantial amount of background details in this section. The expert reader may wish to skim or skip this section, returning only if questions arise in subsequent sections.

4.1. Polyhedral theory. We let $0_d \in \mathbb{R}^d$ denote the vector of zeros, $\mathbf{1}_n \in \mathbb{R}^n$ the vector of ones, and $I_d \in \mathbb{R}^{d \times d}$ the identity matrix; when dimensions are clear from context, we suppress subscripts. The vectorized signum function $\text{sign} : \mathbb{R}^d \rightarrow \{-1, +1\}^d$ is defined by

$$(4.1) \quad \forall x \in \mathbb{R}^d, j \in \{1, \dots, d\} : [\text{sign}(x)]_j = \text{sign}(x_j) = \begin{cases} -1, & x_j < 0; \\ +1, & x_j \geq 0 \end{cases}.$$

⁶e.g. initial condition $((x_0, y_0, \theta_0), (\dot{x}_0, \dot{y}_0, \dot{\theta}_0)) = ((0, h, 0), (0, 0, 0))$ where h is the initial body height

⁷Sourcecode that verifies this fact using a computer algebra system is provided in SM.

⁸Although we introduce this logic purely for illustrative purposes, we note that non-trivial dependence of forcing on the set of active constraints could be implemented physically using clutches [8] or actuators [38].

If $A \in \mathbb{R}^{\ell \times m}$ and $B \in \mathbb{R}^{m \times n}$ then $A \cdot B \in \mathbb{R}^{\ell \times n}$ denotes matrix multiplication. Given a subset $S \subset \mathbb{R}^d$, we define [36, Sec. 2.1.1]

$$(4.2a) \quad \text{aff } S = \left\{ \sum_{j=1}^n \alpha_j v_j : n \in \mathbb{N}, \{v_j\}_{j=1}^n \subset S, \{\alpha_j\}_{j=1}^n \subset \mathbb{R}, \sum_{j=1}^n \alpha_j = 1 \right\},$$

$$(4.2b) \quad \text{cone } S = \left\{ \sum_{j=1}^n \alpha_j v_j : n \in \mathbb{N}, \{v_j\}_{j=1}^n \subset S, \{\alpha_j\}_{j=1}^n \subset [0, \infty) \right\},$$

$$(4.2c) \quad \text{conv } S = \left\{ \sum_{j=1}^n \alpha_j v_j : n \in \mathbb{N}, \{v_j\}_{j=1}^n \subset S, \{\alpha_j\}_{j=1}^n \subset [0, 1], \sum_{j=1}^n \alpha_j = 1 \right\},$$

termed the *affine span*, *cone span*, and *convex hull* of S , respectively. The *dimension* of a convex set S is defined to be the dimension of its affine span, $\dim S = \dim \text{aff } S$. A nonempty set $S \subset \mathbb{R}^d$ is called a *polyhedron* [36, Sec. 2.1.2] if there exists $A \in \mathbb{R}^{m \times d}$, $b \in \mathbb{R}^m$ such that $S = \{x \in \mathbb{R}^d : A \cdot x \leq b\}$; note that S is closed and convex. The linear subspace $\mathcal{L} = \{x \in \mathbb{R}^d : A \cdot x = 0\}$ is called the *lineality space* of S .

4.2. Piecewise-affine functions. We will represent a piecewise-affine function using a *triangulation* (Z^-, Z^+, Δ) [15, Sec. 3.1] that consists of a combinatorial simplicial complex Δ whose vertex set is in 1-to-1 correspondence with each of the finite sets of vectors $Z^- \subset \mathbb{R}^d$, $Z^+ \subset \mathbb{R}^c$. For our purposes,⁹ a *combinatorial simplicial complex* Δ is a collection of finite sets $\Delta = \{\Delta_\omega\}_{\omega \in \Omega}$ such that $S \subset \Delta_\omega \implies S \in \Delta$ for all $\omega \in \Omega$; we call $\bigcup_{\omega \in \Omega} \Delta_\omega$ the *vertex set* of Δ . We assume that, for every $\omega \in \Omega$, the collections of vectors $Z_\omega^\pm \subset Z^\pm$ determined by Δ_ω are *affinely independent* [15, Sec. 2.1.1] so that $\Delta_\omega^\pm = \text{conv } Z_\omega^\pm$ are $(\#(\Delta_\omega) - 1)$ -dimensional geometric simplices [15, Claim 2.9] where $\Delta_\omega^- \subset \mathbb{R}^d$, $\Delta_\omega^+ \subset \mathbb{R}^c$. We assume further that, for every $\omega, \omega' \in \Omega$, the collections of vectors $Z_{\omega, \omega'}^\pm \subset Z^\pm$ determined by $\Delta_\omega \cap \Delta_{\omega'}$ coincide with $Z_\omega^\pm \cap Z_{\omega'}^\pm \subset Z^\pm$ so that $\Delta^\pm = \{\Delta_\omega^\pm\}_{\omega \in \Omega}$ are *geometric simplicial complexes* [15, Sec. 2.2.1]. With these assumptions in place, the correspondence between Z^- and Z^+ determined by the triangulation (Z^-, Z^+, Δ) uniquely defines a piecewise-affine function $P : |\Delta^-| \rightarrow |\Delta^+|$ using the construction from [15, Sec. 3.1] where $|\Delta^-| = \bigcup_{\omega \in \Omega} \Delta_\omega^- \subset \mathbb{R}^d$, $|\Delta^+| = \bigcup_{\omega \in \Omega} \Delta_\omega^+ \subset \mathbb{R}^c$ are termed the *carriers* [36, Sec. 2.2.1] of the geometric simplicial complexes Δ^\pm .

4.3. Piecewise-linear functions. If a piecewise-affine function $P : \mathbb{R}^d \rightarrow \mathbb{R}^c$ is *positively homogeneous*, that is,

$$(4.3) \quad \forall \alpha \geq 0, v \in \mathbb{R}^d : P(\alpha \cdot v) = \alpha \cdot P(v),$$

then P is *piecewise-linear* [36, Prop. 2.2.1]. In this case, P admits a *conical subdivision* [36, Prop. 2.2.3], that is, there exists a finite collection $\Sigma = \{\Sigma_\omega\}_{\omega \in \Omega}$ such that: (i) $\Sigma_\omega \subset \mathbb{R}^d$ is a d -

⁹There are more general definitions of ([complete] semi-)simplicial complexes and the closely-related concept of Δ -complexes in the literature [16, Ch. 2.1], [15, App. A.3.1]. Since we employ these concepts primarily in service of parameterizing piecewise-affine functions as in [15, Sec. 3.1], we adopt the (relatively restrictive) definitions of *combinatorial* and *geometric* simplicial complexes from [15, Sec. 2.2.1] in what follows.

dimensional *polyhedral cone* for each $\omega \in \Omega$;¹⁰ (ii) the Σ_ω 's cover \mathbb{R}^d ;¹¹ and (iii) the intersection $\Sigma_\omega \cap \Sigma_{\omega'}$ is either empty or a *proper face* of both polyhedral cones for each $\omega, \omega' \in \Omega$.¹²

4.4. Piecewise-differentiable (PC^r) functions. (This section is largely repeated from [6, Sec. 3.2].) The notion of piecewise-differentiability we employ was originally introduced in [32]; since the monograph [36] provides a more recent and comprehensive exposition, we adopt the notational conventions therein. Let $r \in \mathbb{N} \cup \{\infty\}$ and $D \subset \mathbb{R}^d$ be open. A continuous function $f : D \rightarrow \mathbb{R}^c$ is called *piecewise- C^r* if for every $x_0 \in D$ there exists an open set $U \subset D$ containing x_0 and a finite collection $\{f_j : U \rightarrow \mathbb{R}^c\}_{j \in J}$ of C^r functions such that for all $x \in U$ we have $f(x) \in \{f_j(x)\}_{j \in J}$. The functions $\{f_j\}_{j \in J}$ are called *selection functions* for $f|_U$, and f is said to be a *continuous selection* of $\{f_j\}_{j \in J}$ on U . A selection function f_j is said to be *active* at $x \in U$ if $f(x) = f_j(x)$. We let $PC^r(D, \mathbb{R}^c)$ denote the set of piecewise- C^r functions from D to \mathbb{R}^c . Note that PC^r is closed under composition. The definition of piecewise- C^r may at first appear unrelated to the intuition that a function ought to be piecewise-differentiable precisely if its “domain can be partitioned locally into a finite number of regions relative to which smoothness holds” [33, Section 1]. However, as shown in [33, Thm. 2], piecewise- C^r functions are always piecewise-differentiable in this intuitive sense.

Piecewise-differentiable functions possess a first-order approximation $Df : TD \rightarrow T\mathbb{R}^c$ called the *Bouligand derivative* (or B-derivative) [36, Ch. 3]; this is the content of [36, Lemma 4.1.3]. Significantly, this B-derivative obeys generalizations of many techniques familiar from calculus, including the Chain Rule [36, Thm 3.1.1], Fundamental Theorem of Calculus [36, Prop. 3.1.1], and Implicit Function Theorem [31, Cor. 20]. We let $Df(x; \delta x)$ denote the B-derivative of f evaluated on the tangent vector $\delta x \in T_x D$. The B-derivative is positively homogeneous, i.e. $\forall \delta x \in T_x D, \lambda \geq 0 : Df(x; \lambda \delta x) = \lambda Df(x; \delta x)$, and coincides with the directional derivative of f in the $\delta x \in T_x D$ direction. In addition, the B-derivative $Df(x) : T_x D \rightarrow T_{f(x)} \mathbb{R}^c$ of f at $x \in D$ is a continuous selection of the derivatives of the selection functions active at x [36, Prop. 4.1.3],

$$(4.4) \quad \forall \delta x \in T_x D : Df(x; \delta x) \in \{Df_j(x) \cdot \delta x\}_{j \in J}.$$

However, the function Df is generally *not* continuous at $(x, \delta x) \in TD$; if it is, then f is C^1 at x [36, Prop. 3.1.2].

4.5. Event-selected C^r (EC^r) vector fields and their PC^r flows. Vector fields with discontinuous right-hand-sides and their associated flows have been studied extensively [14]. In [Definition 2.1](#) [6, Defs. 1, 2], a special class of so-called *event-selected C^r (EC^r)* vector fields were defined which are allowed to be discontinuous along a finite number of codimension-1 submanifolds but do not exhibit *sliding* [20] along these submanifolds, and are C^r elsewhere. Importantly, as shown in [6, Thm. 5], an event-selected C^r vector field $F : \mathbb{R}^d \rightarrow T\mathbb{R}^d$ generates a piecewise-differentiable flow, that is, there exists a function $\phi : \mathcal{F} \rightarrow \mathbb{R}^d$ that is *piecewise- C^r* ($\phi \in PC^r$) in the sense defined in [36, Sec. 4.1] (summarized in [subsection 4.4](#)) where

¹⁰i.e. $\Sigma_\omega = \left\{ \sum_{j=1}^{\ell_\omega} \alpha_j v_j^\omega : \{\alpha_j\}_{j=1}^{\ell_\omega} \subset [0, \infty) \right\}$, some $\{v_j\}_{j=1}^{\ell_\omega} \subset \mathbb{R}^d$ [36, Thm. 2.1.1], and $\dim \Sigma_\omega = d$

¹¹i.e. $\bigcup_{\omega \in \Omega} \Sigma_\omega = \mathbb{R}^d$

¹²i.e. $\Sigma_\omega \cap \Sigma_{\omega'} = \left\{ \sum_{j=1}^{\ell_{\omega, \omega'}} \alpha_j v_j^{\omega, \omega'} : \{\alpha_j\}_{j=1}^{\ell_{\omega, \omega'}} \subset [0, \infty) \right\}$, some $\{v_j^{\omega, \omega'}\}_{j=1}^{\ell_{\omega, \omega'}} \subset \{v_j^\omega\}_{j=1}^{\ell_\omega} \cup \{v_j^{\omega'}\}_{j=1}^{\ell_{\omega'}}$

$\mathcal{F} \subset \mathbb{R} \times \mathbb{R}^d$ and

$$(4.5) \quad \forall (t, x) \in \mathcal{F} : \phi(t, x) = x + \int_0^t F(\phi(s, x)) ds.$$

Since ϕ is PC^r , it admits a first-order approximation $D\phi : T\mathcal{F} \rightarrow T\mathbb{R}^d$ termed the *Bouligand* (or *B-*)derivative [36, Sec. 3.1], which is a continuous piecewise-linear function of tangent vectors at every $(t, x) \in \mathcal{F}$, that is, the directional derivative $D\phi(t, x) : T_{(t,x)}\mathcal{F} \rightarrow T_{\phi(t,x)}\mathbb{R}^d$ is continuous and piecewise-linear for all $(t, x) \in \mathcal{F}$.

4.6. B-derivative of an EC^r vector field's PC^r flow. Suppose $F : \mathbb{R}^d \rightarrow T\mathbb{R}^d$ is an EC^r vector field with PC^r flow $\phi : \mathcal{F} \rightarrow \mathbb{R}^d$. Given a tangent vector $(\delta t, \delta x) \in T_{(t,x)}\mathcal{F}$, it was shown in [6, Sec. 7.1.4] that the value of the B-derivative $D\phi(t, x; \delta t, \delta x) \in T_{\phi(t,x)}\mathbb{R}^d$ can be obtained by solving a jump-linear-time-varying differential equation [6, Eqn. (70)], where the “jump” arises from a matrix Ξ_ω determined by the sequence ω in which the perturbed initial state $x + \alpha \delta x$ crosses the surfaces of discontinuity of the vector field F for small $\alpha > 0$ [6, Eqn. (67)]. However, [6] did not provide a representation of the piecewise-linear operator $D\phi(t, x)$ (and, to the best of our knowledge, neither has subsequent work). The key theoretical contribution of this paper, obtained in section 5, is a representation of the B-derivative with respect to state, $D_x\phi(t, x)$, using a *triangulation* of its domain and codomain as defined in [15, Sec. 3.1] (and recalled in subsection 4.2).

To inform the triangulation of the B-derivative $D_x\phi(t, x)$, we recall the values it takes on. Since the flow $\phi : \mathcal{F} \rightarrow \mathbb{R}^d$ is piecewise- C^r (PC^r), it is a *continuous selection* of a finite collection of C^r functions $\{\phi_\omega : \mathcal{F}_\omega \rightarrow \mathbb{R}^d\}_{\omega \in \Omega}$ near $(t, x) \in \mathcal{F}$, where $\mathcal{F}_\omega \subset \mathcal{F}$ is an open set containing (t, x) for each $\omega \in \Omega$ [36, Sec. 4.1], and the B-derivative $D_x\phi(t, x)$ is a continuous selection of the classical (*Fréchet* or *F-*)derivatives $\{D_x\phi_\omega(t, x)\}_{\omega \in \Omega}$ [36, Prop. 4.1.3], that is,

$$(4.6) \quad \forall \delta x \in W_\omega \subset T_x\mathbb{R}^d : D_x\phi(t, x; \delta x) = D_x\phi_\omega(t, x) \cdot \delta x,$$

where $W_\omega \subset T_x\mathbb{R}^d$ is the subset of tangent vectors where the selection function $D_x\phi_\omega$ is *essentially active* [36, Prop. 4.1.1]. If $s, t \in \mathbb{R}$ and $x \in \mathbb{R}^d$ are such that $0 < s < t$ and the vector field F is C^r on $\phi([0, t] \setminus \{s\}, x)$, i.e. the trajectory initialized at $x \in \mathbb{R}^d$ encounters exactly one discontinuity of F at $\rho = \phi(s, x)$ on the time interval $[0, t]$, then $D_x\phi_\omega(t, x)$ has the form

$$(4.7) \quad D_x\phi_\omega(t, x) = D_x\phi(t - s, \rho) \cdot [F_{+1}(\rho) \quad I_d] \cdot \Xi_\omega \cdot \begin{bmatrix} 0_d^\top \\ I_d \end{bmatrix} \cdot D_x\phi(s, x)$$

where F_{+1} is the C^r extension of $F|_{\text{Int } D_{+1}}$ that exists by virtue of condition 2 in Def. 2.1 and $\Xi_\omega \in \mathbb{R}^{(d+1) \times (d+1)}$ is the matrix from [6, Eqn. (67)] corresponding to the selection function index $\omega \in \Omega$. In what follows, we will work in circumstances where the selection functions are indexed by the symmetric permutation group over n elements, i.e. $\Omega = S_n$, and combine (4.6) and (4.7) as

$$(4.8) \quad \forall \delta x \in W_\sigma \subset T_x\mathbb{R}^d : D_x\phi(t, x; \delta x) = D_x\phi(t - s, \rho) \cdot M_\sigma \cdot D_x\phi(s, x) \cdot \delta x$$

where the *saltation matrix*¹³ $M_\sigma \in \mathbb{R}^{d \times d}$ corresponding to index σ is defined by

$$(4.9) \quad M_\sigma = [F_{+1}(\rho) \quad I_d] \cdot \Xi_\sigma \cdot \begin{bmatrix} 0_d^\top \\ I_d \end{bmatrix}.$$

4.7. Local approximation of an EC^r vector field. Suppose vector field $F : \mathbb{R}^d \rightarrow T\mathbb{R}^d$ is event-selected C^r with respect to $h \in C^r(U, \mathbb{R}^n)$ at $\rho \in U \subset \mathbb{R}^d$. For $b \in B_n = \{-1, +1\}^n$ let

$$(4.10) \quad \tilde{D}_b = \left\{ x \in \mathbb{R}^d : b_j Dh_j(\rho)(x - \rho) \geq 0 \right\}$$

and consider the piecewise-constant vector field $\tilde{F} : \mathbb{R}^d \rightarrow T\mathbb{R}^d$ defined by

$$(4.11) \quad \forall b \in B_n, x \in \tilde{D}_b : \tilde{F}(x) = F_b(\rho)$$

where F_b is the C^r extension of $F|_{\text{Int } D_b}$ that exists by virtue of condition 2 in Def. 2.1¹⁴ Note that \tilde{F} is event-selected C^r with respect to the affine function \tilde{h} defined by

$$(4.12) \quad \forall x \in \mathbb{R}^d : \tilde{h}(x) = Dh(\rho)(x - \rho),$$

whence it generates a piecewise-differentiable flow $\tilde{\phi} : \tilde{\mathcal{F}} \rightarrow \mathbb{R}^d$ where $\tilde{\mathcal{F}} = \mathbb{R} \times \mathbb{R}^d$. In [6, Sec. 7.1.3], \tilde{F} was referred to as the *sampled* vector field since it is obtained by ‘‘sampling’’ the selection functions F_b that define F near ρ , and it was noted that the function $\tilde{\phi}$ is piecewise-affine and it approximates the original vector field’s flow ϕ near ρ . We will leverage the algebraic properties of $\tilde{\phi}$ and its relationship to ϕ in what follows to obtain our results.

4.8. Time-to-impact for an EC^r vector field and its local approximation. Suppose vector field $F : \mathbb{R}^d \rightarrow T\mathbb{R}^d$ is event-selected C^r with respect to $h \in C^r(U, \mathbb{R}^n)$ at $\rho \in U \subset \mathbb{R}^d$, and let $\phi \in PC^r(\mathcal{F}, \mathbb{R}^d)$ be its piecewise-differentiable flow. Then [6, Thm. 7] ensures there exists a piecewise-differentiable *time-to-impact* function $\tau \in PC^r(U, \mathbb{R}^n)$ for which

$$(4.13) \quad \forall x \in U, j \in \{1, \dots, n\} : \phi(\tau_j(x), x) \in H_j = h_j^{-1}(h_j(\rho)),$$

i.e. the point x flows to the surface H_j in time $\tau_j(x)$. Similarly, applying [6, Thm. 7] to the sampled vector field $\tilde{F} : \mathbb{R}^d \rightarrow T\mathbb{R}^d$ and piecewise-affine flow $\tilde{\phi} : \tilde{\mathcal{F}} \rightarrow \mathbb{R}^d$ associated with F at ρ constructed in subsection 4.7 ensures there exists a piecewise-affine time-to-impact function $\tilde{\tau} : \mathbb{R}^d \rightarrow \mathbb{R}^n$ for which

$$(4.14) \quad \forall x \in \mathbb{R}^d, j \in \{1, \dots, n\} : \tilde{\phi}(\tilde{\tau}_j(x), x) \in \tilde{H}_j = \rho + \ker Dh_j(\rho),$$

i.e. the point x flows to the affine subspace \tilde{H}_j in time $\tilde{\tau}_j(x)$.

¹³ $\Xi_\sigma \in \mathbb{R}^{(d+1) \times (d+1)}$ is referred to as a saltation matrix in [6, Sec. 7.1.4], but this usage is inconsistent with the original definition of $M_\sigma \in \mathbb{R}^{d \times d}$ as the saltation matrix in [2].

¹⁴Note that \tilde{F} is well-defined as the value of F_b is uniquely determined at ρ by virtue of being continuous, even though the original F is undefined at ρ .

5. Representation. Our main theoretical result is an explicit representation for the Bouligand (or B-)derivative of the piecewise-differentiable flow generated by an event-selected C^r vector field. To that end, let $F : \mathbb{R}^d \rightarrow T\mathbb{R}^d$ be an event-selected C^r vector field and $\phi : \mathcal{F} \rightarrow \mathbb{R}^d$ its piecewise-differentiable flow. In what follows, we will assume that $s, t \in \mathbb{R}$ and $x \in \mathbb{R}^d$ are such that $0 < s < t$ and the vector field F is C^r on $\phi([0, t] \setminus \{s\}, x)$. Although a general trajectory can encounter more than one point of discontinuity for F , such points are isolated [6, Lem. 6], so the Chain Rule for B-differentiable functions [36, Thm. 3.1.1] can be applied to triangulate the desired flow derivative by composing the triangulated flow derivatives associated with each point. Thus, without loss of generality, we restrict our attention to portions of trajectories that encounter one point of discontinuity for F , which point lies at the intersection of n surfaces of discontinuity for F . We assume $n > 1$ because at least two surfaces are needed for our results to be useful: when $n = 1$ the desired B-derivative is linear [2], so it may be represented and employed in computations as a matrix.

The B-derivative $D_x\phi(t, x) : T_x\mathbb{R}^d \rightarrow T_{\phi(t, x)}\mathbb{R}^d$ we seek is a continuous piecewise-linear function, so it can be parsimoniously represented using a *triangulation* [15, Sec. 3.1], that is, a combinatorial simplicial complex (as defined in subsection 4.2) each of whose vertices are associated with a pair of (tangent) vectors – one each in the domain and codomain of $D_x\phi(t, x)$. We will obtain this triangulation via an indirect route: in subsection 5.1, we triangulate the piecewise-affine flow $\tilde{\phi}$ introduced in subsection 4.7; in subsection 5.2, we differentiate our representation of $\tilde{\phi}$ to obtain a triangulation of the B-derivative $D_x\tilde{\phi}$; in subsection 5.3, we show how the B-derivative $D_x\phi$ can be obtained from $D_x\tilde{\phi}$, providing a triangulation of the desired derivative.

5.1. Triangulation. The goal of this subsection is to triangulate the piecewise-affine flow $\tilde{\phi}$ introduced in subsection 4.7. To that end, let $\rho = \phi(s, x)$ and suppose¹⁵ $\text{rank } Dh(\rho) = n$ so $\{\delta\rho \in T_\rho\mathbb{R}^d : b = \text{sign } Dh(\rho) \cdot \delta\rho\}$ has nonempty interior for each $b \in \{-1, +1\}^n = B_n$. Letting $\mathcal{K} = \ker Dh(\rho) \subset T_\rho\mathbb{R}^d$ denote the kernel of $Dh(\rho)$ and \mathcal{K}^\perp its orthogonal complement, for each $b \in B_n$ there exists a unique^{16,17} $\zeta_b \in \mathcal{K}^\perp + \{\rho\}$ such that

$$(5.1) \quad Dh_{b>0}(\rho)(\zeta_b - \rho) = 0 \text{ and } Dh_{b<0}(\rho)(\zeta_b + F_b(\rho) - \rho) = 0$$

where $h_{b>0}$ (respectively, $h_{b<0}$) denotes the function obtained by selecting components h_j of h for which $b_j = +1$ (respectively, $b_j = -1$). The vectors defined by (5.1) have special significance for the piecewise-affine flow $\tilde{\phi}$ introduced in subsection 4.7 (see Figure 5.1(a)):

$$(5.2) \quad \forall b \in B_n : \zeta_b \in \tilde{D}_{-1}, \tilde{\phi}(1, \zeta_b) = \zeta_b + F_b(\rho) \in \tilde{D}_{+1},$$

that is, the point ζ_b lies “before” all event surface tangent planes and flows in 1 (one) unit of time to $\zeta_b + F_b(\rho)$ which lies “after” all event surface tangent planes (neither “before” nor “after” should be interpreted strictly). We denote the collections of these vectors as follows:

$$(5.3) \quad Z^- = \{\zeta_b\}_{b \in B_n}, \quad Z^+ = \{\zeta_b + F_b(\rho)\}_{b \in B_n}.$$

¹⁵As observed in [6, Sec. 7.1.5], first-order approximations of an EC^r vector field’s PC^r flow are not affected by flow between surfaces that are tangent at ρ , so we assume such redundancy has been removed.

¹⁶Here and in what follows we mildly abuse notation via the natural vector space isomorphism $\mathbb{R}^d \simeq T_\rho\mathbb{R}^d$.

¹⁷Uniqueness is ensured by $\text{rank } Dh(\rho) = n$ since (i) \mathcal{K}^\perp is n -dimensional, (ii) the rows of $Dh(\rho)$ are linearly independent, and hence (iii) there are n independent equations in the n unknowns needed to specify ζ_b in (5.1).

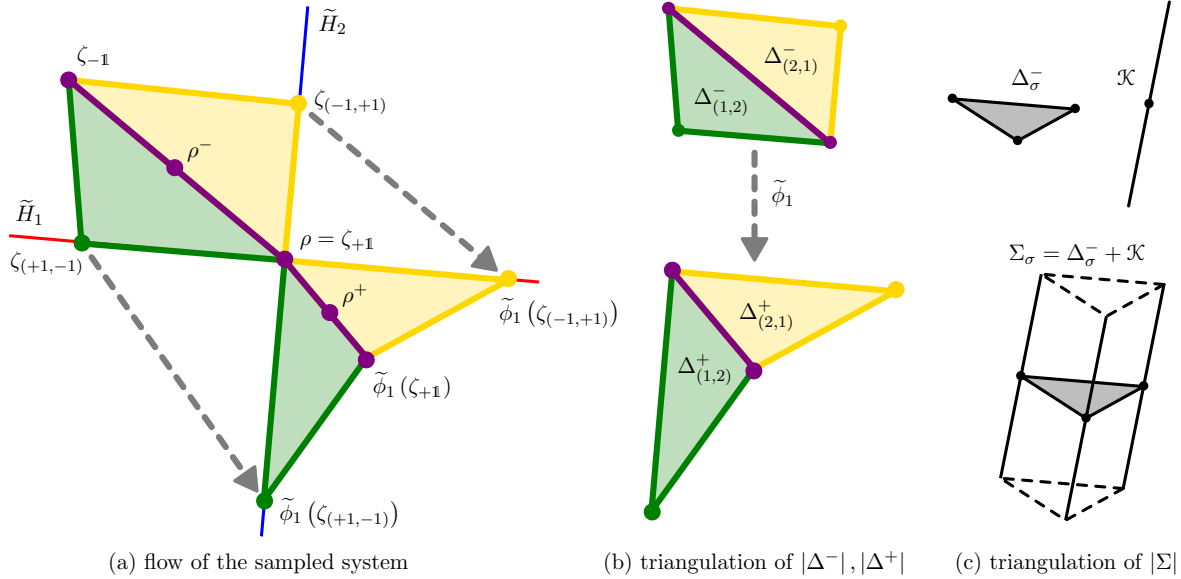


Figure 5.1. Triangulation of the time-1 flow $\tilde{\phi}_1$ of the sampled system associated with an EC^r vector field. (a) For each $b \in \{-1, +1\}^2$, the point ζ_b defined by (5.1) flows from \tilde{D}_{-1} to \tilde{D}_{+1} in 1 (one) unit of time via the sampled system illustrated in Figure 2.1(b) and defined in subsection 4.7. (b) The sets $\{\zeta_{-1}, \zeta_{+1}, \zeta_{(+1,-1)}\}$, $\{\zeta_{-1}, \zeta_{+1}, \zeta_{(-1,+1)}\}$ indexed by (5.5) define geometric simplices $\Delta_{(1,2)}^-$, $\Delta_{(2,1)}^+$ that pass through subspaces \tilde{H}_1, \tilde{H}_2 in the same order. (c) For each $\sigma \in \{(1,2), (2,1)\}$, extending Δ_σ^- by direct sum with subspace \mathcal{K} yields Σ_σ .

In what follows, it will be convenient to use an element $\sigma \in S_n$ of the symmetric permutation group over n elements to specify $n + 1$ elements of $b \in B_n$ as follows: for each $k \in \{0, \dots, n\}$, let $\sigma(\{0, \dots, k\}) \subset \{1, \dots, n\}$ specify the unique $b \in B_n$ whose j -th component is $+1$ if and only if $j \in \sigma(\{0, \dots, k\})$. Note that this identification yields, with some abuse of notation, $\sigma(\{0\}) = -\mathbf{1}$, $\sigma(\{0, \dots, n\}) = +\mathbf{1}$. Finally, note that:

$$(5.4a) \quad \{\zeta_{\sigma(\{0, \dots, k\})} - \rho\}_{k=0}^{n-1} \text{ are linearly independent;}$$

$$(5.4b) \quad \{\zeta_{\sigma(\{0, \dots, k\})} + F_{\sigma(\{0, \dots, k\})}(\rho) - \rho\}_{k=1}^n \text{ are linearly independent.}$$

The former fact (5.4a) is easily verified in coordinates where $Dh(\rho) = [I_n \ 0_{n \times (d-n)}]$, whence the latter fact (5.4b) follows from (5.4a) and (5.2) via [6, Cor. 5(c)] (the time- t flow of an EC^r vector field is a homeomorphism of the state space for all $t \in \mathbb{R}$).

Let Δ denote the combinatorial simplicial complex over vertex set B_n whose maximal n -simplices are indexed by $\sigma \in S_n$ via

$$(5.5) \quad \Delta_\sigma = \{\sigma(\{0, \dots, k\})\}_{k=0}^n \in \Delta$$

where we regard $\sigma(\{0, \dots, k\})$ as an element of B_n using the same abuse of notation employed in (5.4). By associating each vertex $b \in B_n$ with the vector $\zeta_b \in Z^- \subset \mathbb{R}^d$, every n -simplex Δ_σ determines an n -dimensional geometric simplex $\Delta_\sigma^- \subset \mathbb{R}^d$, the dimensionality of which is ensured by (5.4a); similarly, (5.4b) ensures that associating each $b \in B_n$ with $(\zeta_b + F_b(\rho)) \in$

$Z^+ \subset \mathbb{R}^d$ determines an n -dimensional geometric simplex $\Delta_\sigma^+ \subset \mathbb{R}^d$ from each n -simplex Δ_σ . Refer to [Figure 5.1\(b\)](#) for an illustration when $n = 2$. The triple (Z^-, Z^+, Δ) parameterizes a continuous piecewise-affine homeomorphism $P : |\Delta^-| \rightarrow |\Delta^+|$ using the construction from [\[15, Sec. 3.1\]](#) (summarized in [subsection 4.2](#)), where $|\Delta^\pm| = \bigcup_{\sigma \in S_n} \Delta_\sigma^\pm \subset \mathbb{R}^d$ denote the *carriers* of the geometric simplicial complexes Δ^\pm .

We now show that the piecewise-affine function P constructed above is the non-linear part of the time-1 flow of the sampled system $\tilde{\phi}_1$ restricted to $|\Delta^-|$. For each $\sigma \in S_n$ we extend the n -dimensional geometric simplex Δ_σ^- determined by the n -simplex Δ_σ via direct sum with the $(d-n)$ -dimensional subspace \mathcal{K} to obtain a d -dimensional polyhedron Σ_σ (see [Figure 5.1\(c\)](#)), and let $|\Sigma| = \bigcup_{\sigma \in S_n} \Sigma_\sigma$. Note that \mathcal{K} is a subset of the lineality space of Σ_σ for each $\sigma \in S_n$.

Lemma 5.1. $\tilde{\phi}_1|_{|\Sigma|}$ is piecewise-affine and

$$(5.6) \quad \forall z \in |\Delta^-|, \xi \in \mathcal{K} : \tilde{\phi}_1(z + \xi) = P(z) + \xi.$$

Proof. This proof will proceed in two steps: (i) show that $\tilde{\phi}_1(z) = P(z)$ for all $z \in |\Delta^-|$; (ii) show that $\tilde{\phi}_1(z + \xi) = \tilde{\phi}_1(z) + \xi$ for all $z \in |\Delta^-|, \xi \in \mathcal{K}$.

(i) Recall from [\(5.2\)](#) that $\phi_1|_{Z^-} = P|_{Z^-}$ where Z^- is the vertex set for the geometric simplicial complex Δ^- . For each $\sigma \in S_n$ let $Z_\sigma = \{\zeta_b\}_{b \in \Delta_\sigma}$ denote the vertex set of the n -dimensional geometric simplex Δ_σ^- . Then we claim that each $z \in \Delta_\sigma^-$ passes through the same sequence of transition surfaces as each $\zeta_b \in Z_\sigma$. To verify this claim, we use the piecewise-affine *time-to-impact* function $\tilde{\tau} : \mathbb{R}^d \rightarrow \mathbb{R}^n$ from [subsection 4.8](#). Note that ζ_b impacts affine subspace \tilde{H}_j at time 1 if $b_j = -1$ and at time 0 if $b_j = +1$, i.e.

$$(5.7) \quad \tilde{\tau}_j(\zeta_b) = \begin{cases} 1, & b_j = -1; \\ 0, & b_j = +1. \end{cases}$$

A convex combination $\alpha \zeta_b + (1 - \alpha)\zeta_{b'}$, $\alpha \in (0, 1)$, $b, b' \in \Delta_\sigma$, impacts \tilde{H}_j at time

$$\tilde{\tau}_j(\alpha \zeta_b + (1 - \alpha)\zeta_{b'}) = \begin{cases} 1, & b_j = -1 \wedge b'_j = -1; \\ t \in (0, 1), & (b_j = +1 \wedge b'_j = -1) \vee (b_j = -1 \wedge b'_j = +1); \\ 0, & b_j = +1 \wedge b'_j = +1. \end{cases}$$

More generally, any point $z \in \Delta_\sigma^-$ is a convex combination of the vertices Z_σ , whence it impacts surfaces in the order prescribed by σ :

$$(5.8) \quad \forall z \in \Delta_\sigma^- : 0 \leq \tilde{\tau}_{\sigma(1)}(z) \leq \tilde{\tau}_{\sigma(2)}(z) \leq \dots \leq \tilde{\tau}_{\sigma(n)}(z) < 1.$$

Thus, $\tilde{\phi}_1|_{\Delta_\sigma^-}$ is affine and agrees with $P|_{\Delta_\sigma^-}$. Since $|\Delta^-| = \bigcup_{\sigma \in S_n} \Delta_\sigma^-$, we have $\tilde{\phi}_1|_{|\Delta^-|} = P$.

(ii) We now show that the piecewise-affine map $\tilde{\phi}_1$ is indifferent to $\xi \in \mathcal{K} = \ker Dh(\rho)$:

$$(5.9a) \quad \forall \xi \in \mathcal{K}, z \in |\Delta^-| : \tilde{\phi}_1(z + \xi) = \tilde{\phi}_1(\rho + (z + \xi - \rho))$$

$$(5.9b) \quad = \tilde{\phi}_1(\rho) + D\tilde{\phi}_1(\rho; z + \xi - \rho)$$

$$(5.9c) \quad = \tilde{\phi}_1(\rho) + D\tilde{\phi}_1(\rho; z - \rho) + \xi$$

$$(5.9d) \quad = \tilde{\phi}_1(z) + \xi.$$

Indeed: (5.9a) since $z + \xi = \rho + (z + \xi - \rho)$; (5.9b) since $\tilde{\phi}_1$ is affine on the segment $\{\rho + \alpha(z + \xi - \rho) : \alpha \in [0, 1]\}$; (5.9c) since each piece of the continuous piecewise-linear B-derivative $D\tilde{\phi}_1(\rho)$ is specified by a saltation matrix (as recalled in subsection 4.4) that is the product of matrices of the form $(I_d + g \cdot Dh_j(\rho))$ [6, Eqn. (60)], thus $\xi \in \mathcal{K} = \ker Dh(\rho)$ is transformed by I_d ; (5.9d) for the same reason as (5.9b). ■

5.2. B-derivative of $\tilde{\phi}$. The goal of this subsection is to differentiate the representation of $\tilde{\phi}$ from subsection 5.1 to obtain a triangulation of the B-derivative $D\tilde{\phi}_1 : T_{\rho^-}\mathbb{R}^d \rightarrow T_{\rho^+}\mathbb{R}^d$ between the following two points:

$$(5.10) \quad \rho^- = \rho - \frac{1}{2}F_{-1}(\rho), \quad \rho^+ = \tilde{\phi}(1, \rho^-) = \rho + \frac{1}{2}F_{+1}(\rho).$$

Lemma 5.2. *The function $B = D\tilde{\phi}_1(\rho^-) : T_{\rho^-}\mathbb{R}^d \rightarrow T_{\rho^+}\mathbb{R}^d$ satisfies:*

1. B specifies how $\tilde{\phi}_1$ varies relative to $\tilde{\phi}_1(\rho^-)$,

$$(5.11) \quad \forall x \in |\Sigma| : \tilde{\phi}_1(x) = \tilde{\phi}_1(\rho^-) + B(x - \rho^-);$$

2. B is continuous and piecewise-linear with conical subdivision

$$(5.12) \quad \Sigma' = \{\Sigma'_\sigma = \text{cone}(\Sigma_\sigma - \rho^-) : \sigma \in S_n\};$$

3. $B|_{\Sigma'_\sigma}$ is linear for all $\sigma \in S_n$ and

$$(5.13) \quad \forall \delta\rho \in \Sigma'_\sigma : B(\delta\rho) = M_\sigma \cdot \delta\rho;$$

4. $\mathcal{L} = \mathcal{K} + \text{span } F_{-1}(\rho)$ is a $(d - n + 1)$ -dimensional lineality space for Σ' and

$$(5.14) \quad \forall \sigma \in S_n : \Sigma'_\sigma = \mathcal{L} + \text{cone} \left\{ \Pi_{\mathcal{L}}^\perp \cdot (\zeta_{\sigma(\{0, \dots, k\})} - \rho) \right\}_{k=1}^{n-1},$$

where $\Pi_{\mathcal{L}}^\perp$ is the orthogonal projection onto \mathcal{L}^\perp ;

5. $B|_{\mathcal{L}}$ is linear and

$$(5.15) \quad \forall \delta\rho \in T_{\rho^-}\mathbb{R}^d : B(\delta\rho) = B(\Pi_{\mathcal{L}} \cdot \delta\rho) + B\left(\Pi_{\mathcal{L}}^\perp \cdot \delta\rho\right),$$

where $\Pi_{\mathcal{L}}$ is the orthogonal projection onto \mathcal{L} .

Proof. Each point follows from straightforward application of results in [36]: (1.), (2.), and (3.) are conclusions (4.), (3.), and (2.), respectively, of [36, Prop. 2.2.6]; (4.) follows from the definitions of lineality space [36, Sec. 2.1.2] and the ζ_b 's (5.1); (5.) is a restatement of [36, Lem. 2.3.2]. ■

5.3. B-derivative of ϕ . The goal of this subsection is to show that the piecewise-linear function B triangulated in subsection 5.2 gives the non-linear part of the desired B-derivative $D_x\phi(t, x)$ and¹⁸

$$(5.16) \quad W_\sigma = D_x\phi(s, x)^{-1}(\Sigma'_\sigma) \subset T_x\mathbb{R}^d$$

is the cone of tangent vectors where the saltation matrix M_σ is active in (4.8).

¹⁸Here and in what follows we mildly abuse notation via the natural vector space isomorphisms $\mathbb{R}^d \simeq T_{\rho^-}\mathbb{R}^d \simeq T_{\rho^+}\mathbb{R}^d \simeq T_\rho\mathbb{R}^d$.

Theorem 5.3. *Suppose the vector field $F : \mathbb{R}^d \rightarrow T\mathbb{R}^d$ is event-selected C^r with respect to $h : \mathbb{R}^d \rightarrow \mathbb{R}^n$ at ρ . Let $\phi : \mathcal{F} \rightarrow \mathbb{R}^d$ be the PC^r flow of F and $s, t \in \mathbb{R}$, $x \in \mathbb{R}^d$ be such that $0 < s < t$ and F is C^r on $\phi([0, t] \setminus \{s\}, x) \subset \mathbb{R}^d$. Then with $\rho = \phi(s, x)$, the B-derivative of the flow ϕ with respect to state, $D_x\phi(t, x) : T_x\mathbb{R}^d \rightarrow T_{\phi(t, x)}\mathbb{R}^d$, is given by*

$$(5.17a) \quad \forall \delta x \in T_x\mathbb{R}^d : D_x\phi(t, x; \delta x) = D_x\phi(t - s, \rho) \cdot B(D_x\phi(s, x) \cdot \delta x),$$

$$(5.17b) \quad \forall \delta x \in W_\sigma \subset T_x\mathbb{R}^d : D_x\phi(t, x; \delta x) = D_x\phi(t - s, \rho) \cdot M_\sigma \cdot D_x\phi(s, x) \cdot \delta x,$$

where B is the continuous piecewise-linear function from Lemma 5.2, W_σ is the cone from (5.16), and M_σ is the saltation matrix from (4.9). ■

Proof. Note that (5.17a) follows from (5.17b) by (5.13), and the fact that “pieces” of the B-derivative $D_x\phi(t, x)$ are determined by the collection of saltation matrices $\{M_\sigma\}_{\sigma \in S_n}$ was recalled in subsection 4.4. Thus, to establish (5.17b) what remains to be shown is that M_σ is the active “piece” for all $\delta x \in W_\sigma$, i.e. that $\{W_\sigma\}_{\sigma \in S_n}$ is a conical subdivision for the piecewise-linear operator $D_x\phi(t, x)$, with W_σ as defined in (5.16).

Given $\delta x \in \text{Int } W_\sigma$ let $\delta\rho = D_x\phi(s, x) \cdot \delta x \in \text{Int } \Sigma'_\sigma$ so that

$$(5.18) \quad \tilde{\tau}_{\sigma(1)}(\rho + \delta\rho) < \tilde{\tau}_{\sigma(2)}(\rho + \delta\rho) < \cdots < \tilde{\tau}_{\sigma(n)}(\rho + \delta\rho)$$

where $\tilde{\tau}$ is the time-to-impact function for the sampled system as defined in (4.14). Note that $D_x\phi(t, x)$ is linear on $\text{span } F(x)$,

$$(5.19) \quad \forall \alpha \in \mathbb{R} : D_x\phi(t, x; \delta x + \alpha F(x)) = D_x\phi(t, x; \delta x) + \alpha F(\phi(t, x)),$$

so without loss of generality we may assume $\delta\rho \in \text{Int } \tilde{D}_{-1}$ by translating δx in the $-F(x)$ direction. We claim that, for all $\alpha > 0$ sufficiently small, $\phi(t, x + \alpha \delta x)$ passes through the event surfaces with the same sequence as $\phi(1, \rho + \alpha \delta\rho)$, i.e. that

$$(5.20) \quad \tau_{\sigma(1)}(x + \alpha \delta x) < \tau_{\sigma(2)}(x + \alpha \delta x) < \cdots < \tau_{\sigma(n)}(x + \alpha \delta x),$$

where τ is the time-to-impact function defined in (4.13). To see this, note that

$$(5.21a) \quad \forall k \in \{1, \dots, n\} : \tau_{\sigma(k)}(x + \alpha \delta x) - \tau_{\sigma(k)}(x) = D\tau_{\sigma(k)}(x; \alpha \delta x) + O(\alpha^2)$$

$$(5.21b) \quad = D\tilde{\tau}_{\sigma(k)}(\rho; \alpha \delta\rho) + O(\alpha^2)$$

$$(5.21c) \quad = \tilde{\tau}_{\sigma(k)}(\rho + \alpha \delta\rho) - \tilde{\tau}_{\sigma(k)}(\rho) + O(\alpha^2)$$

where: (5.21a) since τ is PC^r ; (5.21b) since $\delta\rho = D_x\phi(s, x) \cdot \delta x$ and $D\tau(x; \delta x)$, $D\tilde{\tau}(\rho; \delta\rho)$ are determined by the same data, namely, $Dh_{\sigma(k)}(\rho)$ and $F_{-1}(\rho)$; (5.21c) since $\delta\rho \in \Sigma'_\sigma$. Combining the approximation (5.21) with (5.18) yields (5.20) as desired.

We conclude that $\{W_\sigma\}_{\sigma \in S_n}$ is a conical subdivision for the piecewise-linear operator $D_x\phi(t, x)$, which verifies (5.17) and completes the proof. ■

Remark 5.4. The only non-classical part of the B-derivative of the flow in (5.17a) is the piecewise-linear function B . Although there are $n!$ pieces of B in general, we explicitly represent all pieces using a triangulation of 2^n sample points defined in (5.3), achieving a substantial reduction – from factorial to “merely” exponential – of the information needed to represent the first-order approximation of the flow. Note that B implicitly determines the transition sequence σ associated with the perturbation direction δx in (5.17a), whereas this sequence must be explicitly specified to select the appropriate saltation matrix M_σ in (5.17b).

6. Computation. We now attend to the complexity of the computational tasks required to construct or evaluate the B-derivative representation from the preceding section. To that end, let $F : \mathbb{R}^d \rightarrow T\mathbb{R}^d$ be an event-selected C^r vector field with respect to $h \in C^r(\mathbb{R}^d, \mathbb{R}^n)$ and $\phi : \mathcal{F} \rightarrow \mathbb{R}^d$ its piecewise- C^r flow, and assume $s, t \in \mathbb{R}$ and $x \in \mathbb{R}^d$ are such that $0 < s < t$, $\rho = \phi(s, x)$, and the vector field F is C^r on $\phi([0, t] \setminus \{s\}, x)$.

We seek to compute $D_x\phi(t, x; \delta x)$ given $\delta x \in T_x\mathbb{R}^d$. Since (5.17a) from Theorem 5.3 yields

$$(6.1) \quad D_x\phi(t, x; \delta x) = D_x\phi(t - s, x) \cdot B(D_x\phi(s, x) \cdot \delta x)$$

where $B : T_\rho\mathbb{R}^d \rightarrow T_\rho\mathbb{R}^d$, the crux of the computation is

$$(6.2) \quad \delta\rho^+ = B(\delta\rho^-)$$

where $\delta\rho^- = D_x\phi(s, x) \cdot \delta x$. In fact, Lemma 5.2 offers further simplification via (5.15): since $B = B \circ \Pi_{\mathcal{L}} + B \circ \Pi_{\mathcal{L}}^\perp$ where $B \circ \Pi_{\mathcal{L}}$ is the linear function

$$(6.3) \quad B \circ \Pi_{\mathcal{L}} \cdot \delta\rho^- = \left(I_d + (F_{+\mathbb{1}}(\rho) - F_{-\mathbb{1}}(\rho)) \cdot \frac{F_{-\mathbb{1}}(\rho)^\top}{\|F_{-\mathbb{1}}(\rho)\|^2} \right) \cdot \Pi_{\mathcal{L}} \cdot \delta\rho^-,$$

only the piecewise-linear function $B \circ \Pi_{\mathcal{L}}^\perp$ (equivalently, the restriction $B|_{\mathcal{L}^\perp}$) requires special consideration. In what follows, we will assume the following data, needed to construct the *sampled system* illustrated in Figure 2.1(b), is given: linearly-independent normal vectors for the surfaces of discontinuity, i.e. $Dh(\rho) \in \mathbb{R}^{n \times d}$ with rank $Dh(\rho) = n$; limiting values of the vector field at the point of intersection, i.e. $F_b(\rho) \in T_\rho\mathbb{R}^d$ for each $b \in B_n$; and F-derivatives of the continuously-differentiable parts of the flow, i.e. $D_x\phi(s, x), D_x\phi(t - s, x) \in \mathbb{R}^{d \times d}$.

6.1. Constructing the B-derivative. Lemma 5.2 demonstrates that there are $n!$ pieces of the piecewise-linear function B , namely, the collection of saltation matrices $\{M_\sigma\}_{\sigma \in S_n}$ in (5.13) that are active on the corresponding polyhedral cones in the conical subdivision $\Sigma' = \{\Sigma'_\sigma\}_{\sigma \in S_n}$ in (5.12). These polyhedral cones are generated by the 2^{n-1} points $\{\zeta_b : b \in B_n \setminus \{-\mathbb{1}, +\mathbb{1}\}\}$ in (5.14). For each $b \in B_n$, the point $\zeta_b \in \mathcal{K}^\perp + \{\rho\}$ where $\mathcal{K} = \ker Dh(\rho)$ can be determined by solving the n affine equations with n unknowns in (5.1). Given $\sigma \in S_n$, the linear piece $B|_{\mathcal{L}^\perp \cap \Sigma'_\sigma}$ can be constructed using the *saltation matrix* [6, Sec. 7.1.6] since $B(\delta\rho^-) = M_\sigma \cdot \delta\rho^-$ for all $\delta\rho^- \in \mathcal{L}^\perp \cap \Sigma'_\sigma$ where¹⁹

$$(6.4) \quad M_\sigma = \prod_{k=0}^{n-1} \left(I_d + \frac{(F_{\sigma(\{0, \dots, k+1\})}(\rho) - F_{\sigma(\{0, \dots, k\})}(\rho))}{Dh_{\sigma(\{0, \dots, k\})}(\rho) \cdot F_{\sigma(\{0, \dots, k\})}(\rho)} \cdot Dh_{\sigma(\{0, \dots, k\})}(\rho) \right),$$

or using *barycentric coordinates* [15, Eqn. (3.1)] since $B(\delta\rho^-) = Z_\sigma^+ \cdot (Z_\sigma^-)^\dagger \cdot \delta\rho^-$ for all $\delta\rho^- \in \mathcal{L}^\perp \cap \Sigma'_\sigma$ where

$$(6.5) \quad Z_\sigma^\pm = \left[z_{\sigma(\{0,1\})}^\pm \quad z_{\sigma(\{0,1,2\})}^\pm \quad \cdots \quad z_{\sigma(\{0,1,\dots,n-1\})}^\pm \right] \in \mathbb{R}^{d \times (n-1)},$$

¹⁹We mildly abuse notation as in subsection 5.1 by using $\sigma \in S_n$ to specify $n+1$ elements of $b \in B_n$: for each $k \in \{0, \dots, n\}$, we let $\sigma(\{0, \dots, k\}) \subset \{1, \dots, n\}$ specify the unique $b \in B_n$ whose j -th component is +1 if and only if $j \in \sigma(\{0, \dots, k\})$.

$$(6.6) \quad \forall b \in \Delta'_\sigma : z_b^- = \Pi_{\mathcal{L}}^\perp \cdot (\zeta_b - \rho), \quad z_b^+ = B|_{\mathcal{L}^\perp}(z_b^-),$$

$$(6.7) \quad \Delta'_\sigma = \{\sigma(\{0, 1, \dots, k\})\}_{k=1}^{n-1};$$

note that the pseudo-inverse $(Z_\sigma^-)^\dagger$ is injective on $\mathcal{L}^\perp \cap \Sigma'_\sigma$ by (5.4a) and (5.14). Although the matrices $M_\sigma, Z_\sigma^+ \cdot (Z_\sigma^-)^\dagger \in \mathbb{R}^{d \times d}$ define the same linear transformation on the $(n-1)$ -dimensional cone $\mathcal{L}^\perp \cap \Sigma'_\sigma$, they are generally not the same matrix. We conclude by noting that constructing the saltation matrix in (6.4) requires $O(nd^2)$ time and $O(d^2)$ space, whereas constructing the Barycentric coordinates in (6.5) requires $O(n^2d^2)$ time and $O(d^2)$ space (although evaluating the expression $Z_\sigma^+ \cdot (Z_\sigma^-)^\dagger \cdot \delta\rho^-$ requires only $O(nd^2)$ time given Z_σ^\pm).

6.2. Evaluating the B-derivative. One obvious strategy to evaluate B on $\delta\rho^- \in T_\rho\mathbb{R}^d$ is to (i) determine $\sigma \in S_n$ such that $\delta\rho^- \in \Sigma'_\sigma$ then (ii) apply the corresponding saltation matrix or barycentric coordinates calculation from the preceding section. The general formulation of (i), termed the *point location* problem in the computational geometry literature, is “essentially open” [9, Sec. 6.5]. For an arrangement of m hyperplanes in \mathbb{R}^d , queries can be answered in $O(d \log m)$ time at the expense of $O(m^d)$ space [7]. In our context, the conical subdivision Σ' in (5.14) is determined by an arrangement of $m = O(n^2)$ hyperplanes, so this general-purpose algorithm has time complexity $O(d \log n!) = O(dn \log n)$ and space complexity $O(n!^d)$.

The relationship established by (5.11) between the desired B-derivative and the flow of the *sampled system* illustrated in Figure 2.1(b) suggests a different strategy, summarized in Figure 2.2, with slightly worse $O(n^2d)$ time complexity but dramatically superior $O(d)$ space complexity. To understand the strategy, interpret the tangent vector $\delta\rho^- \in T_{\rho^-}\mathbb{R}^d$ as a perturbation away from the point $\rho^- = \rho - \frac{1}{2}F_{-1}(\rho)$ that flows through ρ to $\rho^+ = \rho + \frac{1}{2}F_{+1}(\rho)$ in one unit of time and observe that²⁰ $\delta\rho^+ = \tilde{\phi}_1(\rho^- + \delta\rho^-) - \rho^+ = B(\delta\rho^-)$ as in (5.11). The flow of the sampled system $\tilde{\phi}_1$ is piecewise-affine, and can be evaluated on a given perturbation vector $\delta\rho^-$ by performing a sequence of n affine projections (one for each of the affine subspaces $\{\tilde{H}_j\}_{j=1}^n$ where \tilde{F} is discontinuous) specified by the permutation $\sigma \in S_n$ for which $\delta\rho^- \in \Sigma'_\sigma$. Fortunately, the sequence σ can be determined inductively as follows. First, define

$$(6.8) \quad \begin{aligned} \delta t_1 &= 0, \\ \delta \rho_1 &= \delta \rho^-, \\ \sigma(1) &= \arg \min \left\{ -\frac{Dh_j(\rho) \cdot \delta \rho_1}{Dh_j(\rho) \cdot F_{-1}(\rho)} : j \in \{1, \dots, n\} \right\}, \\ \tau_1 &= -\frac{Dh_{\sigma(1)}(\rho) \cdot \delta \rho_1}{Dh_{\sigma(1)}(\rho) \cdot F_{-1}(\rho)}. \end{aligned}$$

²⁰This equation only holds when $\|\delta\rho^-\|$ is small enough to ensure $\rho^- + \delta\rho^- \in \tilde{D}_{-1}$ and $\rho^+ + \delta\rho^+ \in \tilde{D}_{+1}$; since the B-derivative is positively-homogeneous, we impose this restriction without loss of generality.

Then for $k \in \{1, \dots, n-1\}$ inductively define

$$(6.9) \quad \begin{aligned} \delta t_{k+1} &= \delta t_k + \tau_k, \\ \delta \rho_{k+1} &= \delta \rho_k + \tau_k \cdot F_{\sigma(\{0, \dots, k-1\})}(\rho), \\ \sigma(k+1) &= \arg \min \left\{ -\frac{Dh_j(\rho) \cdot \delta \rho_{k+1}}{Dh_j(\rho) \cdot F_{\sigma(\{0, \dots, k\})}(\rho)} : j \in \{1, \dots, n\} \setminus \sigma(\{1, \dots, k\}) \right\}, \\ \tau_{k+1} &= -\frac{Dh_{\sigma(k+1)}(\rho) \cdot \delta \rho_{k+1}}{Dh_{\sigma(k+1)}(\rho) \cdot F_{\sigma(\{0, \dots, k\})}(\rho)}. \end{aligned}$$

Finally, set $\delta \rho^+ = \delta \rho_n - (\delta t_n + \tau_n) \cdot F_{+1}(\rho)$. By construction, $\delta \rho^- \in \Sigma'_\sigma$ and $\delta \rho^+ = B(\delta \rho^-)$. This strategy is succinctly summarized in pseudocode and sourcecode in Figure 2.2; its time complexity is $O(n^2 d)$ since there are n steps in the induction and each step requires $O(n)$ dot products between d -vectors. The space complexity is $O(d)$ since each step in the induction requires $O(d)$ storage and data from preceding steps can be forgotten or overwritten.

We conclude by noting that, if a general-purpose algorithm is employed to solve the point location problem in $O(dn \log n)$ time to obtain the sequence $\sigma \in S_n$, then the induction described in the preceding paragraph can be simplified by skipping the steps that determine $\sigma(1)$ and $\sigma(k+1)$ from (6.8) and (6.9). This simplification reduces the time complexity of the induction to $O(nd)$, so the overall algorithm retains the $O(dn \log n)$ time complexity of the general-purpose point-location algorithm (at the expense of the superexponential $O(n!^d)$ space complexity of the point location algorithm). We are pessimistic these asymptotic complexities can be improved in general.

7. Conclusion. We constructed a representation for the *Bouligand* (or *B*-)derivative of the *piecewise- C^r* (PC^r) flow generated by an *event-selected C^r* (EC^r) vector field and applied the representation to derive a polynomial-time algorithm to evaluate the B-derivative on a given tangent vector. Our results provide a foundation that may support future work generalizing classical analysis and synthesis techniques for smooth control systems to the class of nonsmooth systems considered here. In particular, we envision applying our results to design and control the class of mechanical systems subject to unilateral constraints that arise in models of robot locomotion and manipulation.

REFERENCES

- [1] J. AGUILAR AND D. I. GOLDMAN, *Robophysical study of jumping dynamics on granular media*, Nature physics, 12 (2015), p. nphys3568, <https://doi.org/10.1038/nphys3568>.
- [2] M. A. AIZERMAN AND F. R. GANTMACHER, *Determination of stability by linear approximation of a periodic solution of a system of differential equations with discontinuous right-hand sides*, The Quarterly Journal of Mechanics and Applied Mathematics, 11 (1958), pp. 385–398, <https://doi.org/10.1093/qjmam/11.4.385>.
- [3] P. BALLARD, *The dynamics of discrete mechanical systems with perfect unilateral constraints*, Archive for Rational Mechanics and Analysis, 154 (2000), pp. 199–274, <https://doi.org/10.1007/s002050000105>.
- [4] D. P. BERTSEKAS, *Nonlinear Programming*, Athena Scientific, 2nd ed., 1999.
- [5] F. BIZZARRI, A. BRAMBILLA, AND G. STORTI GAJANI, *Lyapunov exponents computation for hybrid neurons*, Journal of Computational Neuroscience, 35 (2013), pp. 201–212, <https://doi.org/10.1007/s10827-013-0448-6>.

- [6] S. A. BURDEN, S. S. SASTRY, D. E. KODITSCHKEK, AND S. REVZEN, *Event-selected vector field discontinuities yield piecewise-differentiable flows*, SIAM Journal on Applied Dynamical Systems, 15 (2016), pp. 1227–1267, <https://doi.org/10.1137/15M1016588>.
- [7] B. CHAZELLE AND J. FRIEDMAN, *Point location among hyperplanes and unidirectional ray-shooting*, Computational Geometry, 4 (1994), pp. 53–62, [https://doi.org/10.1016/0925-7721\(94\)90009-4](https://doi.org/10.1016/0925-7721(94)90009-4).
- [8] S. H. COLLINS, M. B. WIGGIN, AND G. S. SAWICKI, *Reducing the energy cost of human walking using an unpowered exoskeleton*, Nature, 522 (2015), pp. 212–215, <https://doi.org/10.1038/nature14288>.
- [9] M. DE BERG, M. VAN KREVELD, M. OVERMARS, AND O. SCHWARZKOPF, *Computational Geometry: Algorithms and Applications*, Springer, 2000.
- [10] M. DI BERNARDO, C. BUDD, A. R. CHAMPNEYS, AND P. KOWALCZYK, *Piecewise-smooth dynamical systems: theory and applications*, vol. 163, Springer Science + Business Media, 2008.
- [11] L. DIECI AND L. LOPEZ, *Fundamental matrix solutions of piecewise smooth differential systems*, Mathematics and Computers in Simulation, 81 (2011), pp. 932–953, <https://doi.org/10.1016/j.matcom.2010.10.012>.
- [12] R. ELANDT, E. DRUMWRIGHT, M. SHERMAN, AND A. RUINA, *A pressure field model for fast, robust approximation of net contact force and moment between nominally rigid objects*, in IEEE/RSJ International Conference on Intelligent Robots and Systems (IROS), Nov. 2019, pp. 8238–8245, <https://doi.org/10.1109/IROS40897.2019.8968548>.
- [13] J. ELDERING AND H. JACOBS, *The role of symmetry and dissipation in biolocomotion*, SIAM Journal on Applied Dynamical Systems, 15 (2016), pp. 24–59, <https://doi.org/10.1137/140970914>.
- [14] A. F. FILIPPOV, *Differential equations with discontinuous righthand sides*, Springer, 1988.
- [15] R. E. GROFF, *Piecewise linear homeomorphisms for approximation of invertible maps*, PhD thesis, University of Michigan, 2003.
- [16] A. HATCHER, *Algebraic topology*, Cambridge University Press, 2002.
- [17] J. P. HESPANHA, *Linear systems theory*, Princeton University Press, 2009.
- [18] I. A. HISKENS AND M. A. PAI, *Trajectory sensitivity analysis of hybrid systems*, IEEE Transactions on Circuits and Systems I: Fundamental Theory and Applications, 47 (2000), pp. 204–220, <https://doi.org/10.1109/81.828574>.
- [19] A. P. IVANOV, *The stability of periodic solutions of discontinuous systems that intersect several surfaces of discontinuity*, Journal of Applied Mathematics and Mechanics, 62 (1998), pp. 677–685, [https://doi.org/10.1016/S0021-8928\(98\)00087-2](https://doi.org/10.1016/S0021-8928(98)00087-2).
- [20] M. R. JEFFREY, *Dynamics at a switching intersection: hierarchy, isonomy, and multiple sliding*, SIAM Journal on Applied Dynamical Systems, 13 (2014), pp. 1082–1105, <https://doi.org/10.1137/13093368X>.
- [21] A. M. JOHNSON, S. A. BURDEN, AND D. E. KODITSCHKEK, *A hybrid systems model for simple manipulation and self-manipulation systems*, The International Journal of Robotics Research, 35 (2016), pp. 1354–1392, <https://doi.org/10.1177/0278364916639380>.
- [22] R. I. LEINE AND H. NIJMEIJER, *Dynamics and bifurcations of non-smooth mechanical systems*, vol. 18, Springer Science + Business Media, 2013.
- [23] L. LJUNG, *System identification: theory for the user*, Prentice-Hall, 1999.
- [24] P. LÖTSTEDT, *Mechanical systems of rigid bodies subject to unilateral constraints*, SIAM Journal on Applied Mathematics, 42 (1982), pp. 281–296, <https://doi.org/10.1137/0142022>.
- [25] T. E. OLIPHANT, *A guide to NumPy*, vol. 1, Trelgol Publishing USA, 2006.
- [26] A. M. PACE AND S. A. BURDEN, *Piecewise-differentiable trajectory outcomes in mechanical systems subject to unilateral constraints*, in Hybrid Systems: Computation and Control (HSCC), 2017, pp. 243–252, <https://doi.org/10.1145/3049797.3049807>.
- [27] T. S. PARKER AND L. O. CHUA, *Practical numerical algorithms for chaotic systems*, Springer, 1989.
- [28] E. POLAK, *Optimization: algorithms and consistent approximations*, Springer-Verlag, 1997.
- [29] L. S. PONTRYAGIN, V. G. BOLTYANSKII, R. V. GAMKRELIDZE, AND E. F. MISHCHENKO, *The mathematical theory of optimal processes (translated by KN Trivogoff)*, John Wiley & Sons, 1962.
- [30] PYTHON SOFTWARE FOUNDATION, *Python language reference, version 3.7*, <https://docs.python.org/release/3.7.0/>.
- [31] D. RALPH AND S. SCHOLTES, *Sensitivity analysis of composite piecewise smooth equations*, Mathematical Programming, 76 (1997), pp. 593–612, <https://doi.org/10.1007/BF02614400>.

- [32] S. M. ROBINSON, *Local structure of feasible sets in nonlinear programming, part III: stability and sensitivity*, *Nonlinear Analysis and Optimization*, 30 (1987), pp. 45–66, <https://doi.org/10.1007/BFb0121154>.
- [33] R. T. ROCKAFELLAR, *A property of piecewise smooth functions*, *Computational Optimization and Applications*, 25 (2003), pp. 247–250, <https://doi.org/10.1023/A:1022921624832>.
- [34] S. SASTRY AND M. BODSON, *Adaptive control: stability, convergence, and robustness*, Prentice Hall, 1989.
- [35] S. S. SASTRY, *Nonlinear Systems: Analysis, Stability, and Control*, Springer, 1999.
- [36] S. SCHOLTES, *Introduction to piecewise differentiable equations*, Springer-Verlag, 2012, <https://doi.org/10.1007/978-1-4614-4340-7>.
- [37] S. N. SIMIC, K. H. JOHANSSON, J. LYGEROS, AND S. SASTRY, *Towards a geometric theory of hybrid systems*, *Dynamics of Continuous, Discrete & Impulsive Systems. Series B. Applications & Algorithms*, 12 (2005), pp. 649–687, <http://www.diva-portal.org/smash/record.jsf?pid=diva2:437188>.
- [38] K. SREENATH, H.-W. PARK, I. POULAKAKIS, AND J. W. GRIZZLE, *A Compliant Hybrid Zero Dynamics Controller for Stable, Efficient and Fast Bipedal Walking on MABEL*, *The International Journal of Robotics Research*, 30 (2011), pp. 1170–1193, <https://doi.org/10.1177/0278364910379882>.
- [39] A. TORNAMBE, *Modeling and control of impact in mechanical systems: theory and experimental results*, *IEEE Transactions on Automatic Control*, 44 (1999), pp. 294–309, <https://doi.org/10.1109/9.746255>.
- [40] V. UTKIN, *Variable structure systems with sliding modes*, *IEEE Transactions on Automatic Control*, 22 (1977), pp. 212–222, <https://doi.org/10.1109/TAC.1977.1101446>.